Image Reconstruction Based on the Anatomical Information for Magnetic Resonance Electrical Impedance Tomography

Liling Hao [1], Lisheng Xu [1,2], Benqiang Yang [3], and Gang Li [4]

[1] Department of Sino-Dutch Biomedical and Information Engineering
Northeastern University, Shenyang, 110169, China
haoll@bmie.neu.edu.cn, xuls@bmie.neu.edu.cn

[2] Key Laboratory of Medical Image Computing (Northeastern University), Ministry of Education, China
xuls@bmie.neu.edu.cn

[3] General Hospital of Shenyang Military, Shenyang, 110016, China
bqyang888@sina.com

[4] College of Precision Instrument and Opto-Electronics Engineering, Tianjin University, 300072, Tianjin, China
ligang59@tju.edu.cn

Abstract ─ Magnetic resonance electrical impedance tomography (MREIT) is a noninvasive modality to visualize the internal electrical conductivity distribution of an electrically conductive object using a magnetic resonance imaging (MRI) scanner. The impedance tomography step may provide valuable additional information that cannot be recovered from the MR reconstruction. Previous research has been mostly performed on the reconstruction algorithms and the measurement system. However, the anatomical information provided by the MR images is not in full use. This paper proposes an image reconstruction method based on anatomical information which provides the prior knowledge. The sensitivity algorithm with generalized minimum residual (GMRES) is proposed to reconstruct conductivity image. Simulations of a realistic geometry leg model are performed to show that our approach is not only capable of achieving high accuracy, but also able to improve the speed of the image reconstruction. At the end, a preliminary phantom experiment is presented, illustrating the feasibility of this proposed method.

Index Terms ─ Anatomical information, image reconstruction, magnetic resonance electrical impedance tomography, prior knowledge.

I. INTRODUCTION

Magnetic resonance electrical impedance tomography (MREIT) is a promising imaging technique that aims to reconstruct the cross-sectional conductivity image with the high spatial resolution by measuring the internal magnetic flux density of injection currents with the magnetic resonance imaging (MRI) scanner [1-4]. As a noninvasive imaging technique, it has potential of becoming a new clinical device for the detection of diagnostically valuable information about the status of human tissue [5]. When current is injected into an object through a pair of surface electrodes, the component of the induced magnetic flux density which parallels the direction of the main magnetic field of a MRI scanner can be obtained by scaling the phase shift in the MR complex images. According to the relationship between the conductivity and the induced magnetic flux density, the conductivity distribution of the imaging object can be reconstructed from the measured magnetic flux density data.

Early MREIT researches attempted to reconstruct the conductivity image based on the current density such as **J**-substitution algorithm [6], CCVSR algorithm [7], and equipotential line method [8]. These current density based algorithms need all three components of the magnetic flux density, where each component of magnetic flux density can be obtained by a single measurement. Thus, for the current density based algorithms, the subject must be rotated twice after its original placement to acquire all three components of the induced magnetic flux density. Recently, some simple and efficient methods were reported [9-16] to reconstruct the conductivity image using the component of a magnetic flux density directly which parallels to the main magnetic field of a MRI scanner, such as sensitivity-based algorithm [9-11], the algebraic reconstruction technique [12], harmonic $\mathbf{B}_z$ algorithm [13-14], gradient $\mathbf{B}_z$ decomposition algorithm [15], response surface methodology algorithm [16]. Among

Submitted On: November 18, 2015
Accepted On: May 3, 2016

these methods, the sensitivity algorithm has received a good evaluation in terms of accuracy and efficiency [17]. Moreover, it is necessary to make the most use of the anatomical information generated from segmented MR images benefit MREIT image reconstruction. The impedance tomography combined with the existing imaging parameter of MRI may provide much more pathological information for the diagnosis of human diseases.

This paper proposes an improved image reconstruction technique based on the anatomical information generated from segmented MR images. The sensitivity algorithm with generalized minimum residual (GMRES) method is utilized to solve the inverse problem of MREIT. The simulation results with a realistic geometry leg model are analyzed for the feasibility of the proposed method. The result of a phantom experiment performed on an Open 0.36T MRI scanner is also presented in this work.

II. METHODS

A. Forward problem of MREIT

The electrical current I is injected into a conductive object Ω through a pair of electrodes fixed to the object's boundary $\partial\Omega$. The relation between conductivity and electric potential satisfies the Laplace equation with the Neumann boundary condition:

$$\begin{cases} \nabla\cdot\sigma\nabla\varphi = 0 & \text{in } \Omega \\ -\sigma\dfrac{\partial\varphi}{\partial\mathbf{n}} = J_I & \text{on } \partial\Omega \end{cases}, \tag{1}$$

where σ is the conductivity distribution, and φ is the electric potential in Ω, $\mathbf{n}$ denotes the unit outward unit normal vector on $\partial\Omega$, J_I is the current density at the boundary $\partial\Omega$. The Neumann boundary condition can be written as :

$$\frac{\partial\varphi}{\partial\boldsymbol{n}} = \begin{cases} I/A_+\,\sigma & \text{on current entrance electrode} \\ -I/A_-\,\sigma & \text{on current exit electrode} \\ 0 & \text{elsewhere} \end{cases}, \tag{2}$$

where A_+ and A_- are the areas of two electrodes.

The most popular numerical solution method—finite element method (FEM) is used to obtain the approximate solution of the partial differential equation (PDE) as in Equation (1). After electric potential distribution φ is found, the computations of electrical field intensity and current density can be expressed as:

$$\begin{aligned} \mathbf{E} &= -\nabla\varphi \\ \mathbf{J} &= \sigma\mathbf{E} \end{aligned}. \tag{3}$$

Once the current density $\mathbf{J}$ is obtained, denoting r as the field point and r' as the source point, the magnetic flux density distribution can be computed according to the Biot-Savart law:

$$\mathbf{B}(r) = \frac{\mu_0}{4\pi}\int_\Omega \mathbf{J}(\mathbf{r}')\times\frac{\mathbf{r}-\mathbf{r}'}{|\mathbf{r}-\mathbf{r}'|^3}d\mathbf{r}'. \tag{4}$$

B. Sensitivity reconstruction algorithm based on the anatomical information

A sensitivity based reconstruction algorithm [9-11] is mainly based on linearization of the variation of magnetic flux density due to conductivity perturbations. It initially assumes a uniform conductivity distribution, and calculates a current density distribution with the FEM method the same with the forward problem of conventional electrical impedance tomography (EIT) [18, 19]. Next, the magnetic flux density $\mathbf{B_0}$ can be described according to the Biot-Savart law. Then, suppose there is a conductivity perturbation $\Delta\sigma$ in the imaging region around the uniform values, the electrical potential is changed by $\Delta\varphi$, and the current density changes correspondingly cause an increment of magnetic flux density as $\mathbf{\Delta B}$. According to the sensitivity reconstruction algorithm, the total matrix equation can be represented as:

$$\Delta\mathbf{B} = \mathbf{S}\Delta\boldsymbol{\sigma}, \tag{5}$$

where $\mathbf{S}$ is the sensitivity matrix. Once $\mathbf{S}$ is obtained, the conductivity perturbation $\Delta\sigma$ causing variation of the magnetic flux density $\mathbf{\Delta B}$ can be solved by equation (5). The element of $\mathbf{S}$ at the i^{th} row and j^{th} column which denotes the increment of magnetic flux density at the i^{th} measurement point due to the conductivity perturbation of the j^{th} element can be calculated by:

$$\begin{aligned} S_{ij} &= -\frac{\mu_0}{4\pi}\int_{\Omega_j}(\nabla\varphi + \sigma_0\frac{\partial\nabla\varphi}{\partial\sigma})\times\frac{\mathbf{r}-\mathbf{r}'}{|\mathbf{r}-\mathbf{r}'|^3}d\mathbf{r}' \\ &= -\frac{\mu_0 v_j}{4\pi}\left(-E_j + \sigma_0\nabla\frac{\partial\varphi}{\partial\sigma}\right)\times\frac{\mathbf{r}-\mathbf{r}'}{|\mathbf{r}-\mathbf{r}'|^3} \end{aligned}. \tag{6}$$

Then the conductivity is calculated with the perturbation $\mathbf{\Delta\sigma}$ as:

$$\boldsymbol{\sigma} = \boldsymbol{\sigma}_0 + \Delta\boldsymbol{\sigma}. \tag{7}$$

The sensitivity reconstruction algorithm initially assumes a uniform conductivity distribution. However, the conductivities of biological tissues vary with different tissues, physiological and pathological states. The tremendous changes of conductivity distributions may lead to the big error of the reconstructed result and the long iteration time. The MREIT system can get the MR image while measuring the internal magnetic flux density of injection currents using a MRI scanner. Therefore, the MR image is segmented to generate the anatomical information. Then the different conductivities of different anatomical structures are set as the initial conductivity distribution according to prior knowledge, the known conductivities of the tissues reported by the researchers.

In the first iteration, the method tries to reconstruct only a single slice of an object from $\mathbf{B}_z$ for only its slices which is the middle slice. Before starting to the second iteration, assign the blurred versions of the middle slice for upper and lower slices. In the result, for second iteration we can calculate current density and also

magnetic flux density more accurately unless the upper or lower slices include very high or low conductivity regions.

Considering that the initial conductivity distribution is similar to the true one, the reconstruction algorithm may take advantage of good stability, fast convergence rate and high accuracy. The algorithm which reconstructs the conductivity distribution with anatomical information is described in detail as Fig. 1.

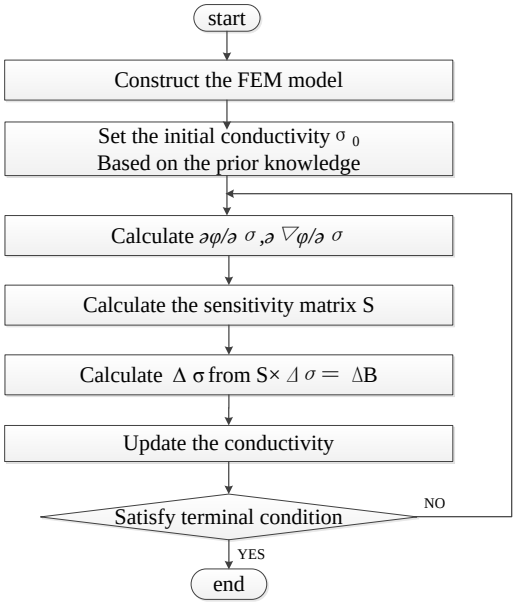

Fig. 1. The flow chart of sensitivity reconstruction algorithm based on the anatomical information.

III. EXPERIMENTS AND RESULTS

A. Simulation results

A realistic geometry model of human leg was constructed for simulation experiment, which was extracted from the realistic MRI magnitude images. The transverse section of the first layer MR magnitude image and the calculation model are shown in Fig. 2 (a) and Fig. 2 (b), respectively. There are four media in the calculation model: fat, muscle, tibia and fibula. And the conductivities of different tissues labelled in Table 1 were set according to the researches published in [20, 21]. The number of slices in MRI scanning is 8, and the size of each voxel is 2 mm × 2 mm × 2 mm. A pair of annular electrodes is located at the first and last slices of the leg model with the electrodes 2 mm width around both ends of the leg model, injecting 10 mA current into the leg model. The model was meshed into hexahedron elements with the size of voxel in MRI. For FEM solution, a mesh structure constructed with tetrahedrons is needed. Therefore, every hexahedron of mesh was subdivided into six tetrahedrons. And each element was assumed to have a uniform conductivity. The FEM mesh for the realistic geometry human leg model is shown in Fig. 2 (c) and Fig. 2 (d). To avoid the inverse crime, the forward problem was calculated on the finer mesh with tetrahedrons elements, while the conductivity images were reconstructed on the coarse mesh with hexahedron elements.

Table 1: Conductivity of different tissues in the model

Tissue	Fat	Skeletal Muscle	Tibia	Fibula
Conductivity (S/m)	0.026	0.5848	0.0057	0.0057

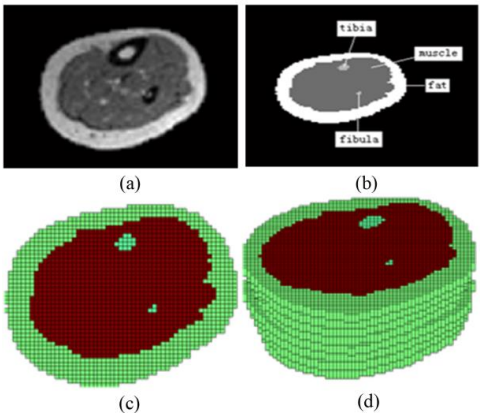

Fig. 2. The calculation model of realistic geometry human leg. (a) The realistic MR image, (b) the calculation model of human leg, (c) top view of the finite element mesh for the model, and (d) three dimensional view of the finite element mesh.

The white Gaussian noise with standard deviation s_B was added to a simulated magnetic flux density data. s_B is given in Equation (8):

$$s_B = 1/\left(2\gamma \times T_c \times SNR_{MR}\right), \tag{8}$$

where γ = 26.75×10^7 radT^{-1}s^{-1} is the gyromagnetic ratio of hydrogen and T_c is the current pulse width in seconds. T_c was set as 50 ms in the simulation experiments. As shown in Equation (8), the standard deviation is inversely proportional to the SNR of the MR magnitude image [22]. In this paper, Gaussian white noise with s_B=0.83405 nT for SNR=70 dB of MR magnitude images was added to the simulated magnetic data.

Figure 3 shows the results of noise added reconstruction for the 3rd-6th slice under the annular electrode mode by sensitivity reconstruction algorithm with the anatomical information and without the anatomical information. The sensitivity reconstruction algorithm based on the anatomical information is observed to yield the better result, which approaches the true conductivity distribution. Moreover, the improved algorithm took 4 iterations and 561.4 s for the reconstruction process, compared to 10 iterations and

2085.8 s for the algorithm based on the uniform conductivity distribution.

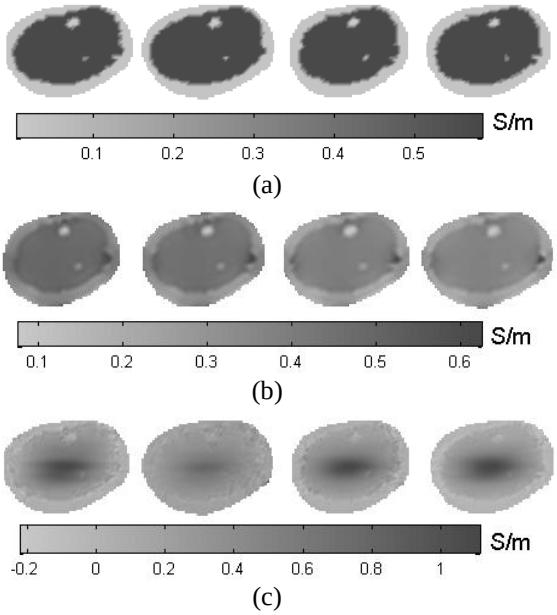

Fig. 3. The results of noise added reconstruction for the 3rd-6th slice under the annular electrode mode. (a) The conductivity image, (b) the reconstructed conductivity image with sensitivity reconstruction algorithm based on the anatomical information, and (c) the reconstructed conductivity image with sensitivity reconstruction algorithm based on the uniform conductivity distribution.

B. Phantom experiment

For a realistic experiment, the current was injected into an imaging object through a pair of annular electrodes attached on a cylindrical phantom shown in Fig. 4. In MREIT imaging, current was injected into an imaging object at the time between a slice select gradient pulse and a read out gradient pulse. An injected current induces a magnetic flux density perturbing the main magnetic field. The perturbation can be calculated from phase differences of MR complex images between one with current injection and another without it.

A cylindrical phantom with 64 mm diameter and 120 mm height was used with a pair of annular carbon electrodes whose widths are 7 mm at the two ends of the phantom as Fig. 3 shows. The phantom was filled with an agar gel (30 g/L NaCl, 1 g/L $CuSO_4$ and 30 g/L agar) to control the T1 and T2 decay of spin density. A piece of pork was immersed in the agar gelatin to create a contrast in both conductivity and spin density. After positioning the phantom inside an Open 0.36 T MRI scanner, the K-space MR data could be collected using the spin pulse sequence. The current injected into the imaging object is 20 mA, and the total current injection time in a TR cycle is 20 ms. The slice thickness is 7 mm with no slice gap, the number of axial slices is 10 at the center of the phantom and TR/TE = 700/59.2 ms. The FOV is 256×256 mm^2 with the matrix size 128×128 and the NEX (number of excitation / acquisition) is 2.

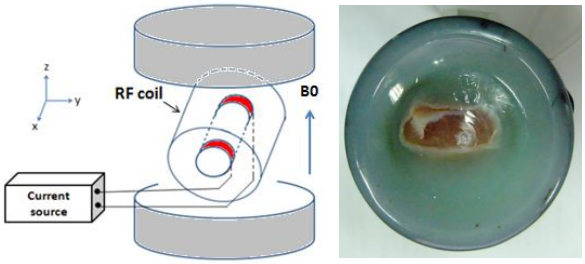

Fig. 4. The phantom experiment for MREIT in an Open MRI scanner. (a) The measurement system, and (b) the phantom with pork.

Using the sensitivity reconstruction algorithm based on the anatomical information, the internal conductivity distribution σ was reconstructed to prove the proposed algorithm. The reconstructed conductivity distribution image is shown in Fig. 5. The pork is shown in Fig. 5 (a) as the darker region in the magnetic resonance magnitude image, which also has a similar contour in Fig. 5 (b). The reconstructed conductivity images with sensitivity reconstruction algorithm based on the uniform conductivity distribution are shown in Fig. 5 (c). The algorithm based on the prior knowledge indeed gives better results than that with the uniform conductivity distribution. In Fig. 5, regarding the reconstruction with experimental data, the improved method is still able to separate the agar and pork, and roughly preserve image boundaries with acceptable background noise. While, one can hardly see anything through the sensitivity reconstruction algorithm based on the uniform conductivity distribution.

The primary experiment result shows the validity of the sensitivity algorithm based on the anatomical information with single current injection under annular electrode mode. Unfortunately, the true conductivity values were not measured, so the reconstructed error will not be discussed.

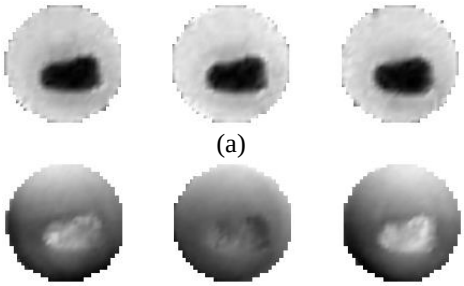

(c)

Fig. 5. The MRI images and reconstructed results of the 3rd-5th slice under the annular electrode mode. (a) Magnetic resonance magnitude image of the phantom, (b) the reconstructed conductivity image sensitivity reconstruction algorithm based on the prior knowledge, and (c) the reconstructed conductivity image with sensitivity reconstruction algorithm based on the uniform conductivity distribution.

IV. CONCLUSION

In this paper, the anatomical information was applied to the inverse problem of magnetic resonance electrical impedance tomography. The sensitivity reconstruction algorithm was used to solve the inverse problem. In the proposed algorithm, the different conductivities of different anatomical structures generated from the segmented MR image are set as the initial conductivity distribution according to the conductivities of the tissues reported by the researchers. Its performance was compared with the sensitivity reconstruction algorithm based on the uniform conductivity distribution. The results of conductivity image reconstructions show that the improved algorithm takes advantage of good stability, fast convergence rate and high accuracy.

This paper utilized the annular electrode mode for an Open MRI scanner whose main magnetic field is perpendicular to the horizontal plane have been widely used in clinical applications for the advantages of its low cost, patient comfort and convenience for interventional treatment. In the annular electrode mode, the distribution of current density component parallels to the main direction of current reflects the distribution of the electrical conductivity. Conductivity images were reconstructed accurately using only one current injection and one component of the magnetic flux density without rotating an image object.

In the modern society, MRI has been one of the most powerful medical imaging modalities currently used. However, the existing MRI parameters are still not enough to diagnose all the diseases accurately. For example, it cannot detect early cancers effectively. And, it can't differentiate calcified tissue. MREIT which aims to image the conductivity distribution is a promising imaging technique to make up for these shortcomings. Moreover, it may provide much more pathological information for the diagnosis of human diseases by combining with the existed imaging parameters. Yet in MREIT, the anatomical information provided by the MR images is not in full use. A sensitivity reconstruction algorithm based on the anatomical information is put forward to improve the quality and speed of image reconstruction. As a new way to improve the conductivity images, the improved algorithm may provide a promising clinical application for MREIT.

ACKNOWLEDGMENTS

This work was supported by the Fundamental Research Funds for the Central Universities (No. N141903002), the National Natural Science Foundation of China (No. 61374015, 61202258), the Ph.D. Programs Foundation of Ministry of Education of China (No. 20110042120037).

REFERENCES

[1] E. J. Woo and J. K. Seo, "Magnetic resonance electrical impedance tomography (MREIT) for high-resolution conductivity imaging," *Physiol. Meas.*, vol. 29, pp. R1-R26, 2008.

[2] H. J. Kim, T. I. Oh, Y. T. Kim, B. I. Lee, E. J. Woo, J. K. Seo, S. Y. Lee, O. Kwon, C. Park, B. T. Kang, and H. M. Park, "In vivo electrical conductivity imaging of a canine brain using a 3 T MREIT system," *Physiol. Meas.*, vol. 29, pp. 1145-1155, 2008.

[3] J. K. Seo, S. W. Kim, S. Kim, J. J. Liu, E. J. Woo, K. Jeon, and C. O. Lee, "Local harmonic Bz algorithm with domain decomposition in MREIT: computer simulation study," *IEEE Trans. Med. Imaging.*, vol. 27, pp. 1754-1761, 2008.

[4] A. Nachman, A. Tamasan, and A. Timonov, "Conductivity imaging with a single measurement of boundary and interior data," *Inverse Problems*, vol. 23, pp. 2551-2563, 2007.

[5] H. M. Park, H. S. Nam, and O. I. Kwon, "Magnetic flux density reconstruction using interleaved partial Fourier acquisitions in MREIT," *Phys. Med. Biol.*, vol. 56, pp. 2059-2073, 2011.

[6] O. Kwon, E. J. Woo, J. R. Yoon, and J. K. Seo, "Magnetic resonance electrical impedance tomography (MREIT): Simulation study of J-substitution algorithm," *IEEE Trans. Biomed. Eng.*, vol. 49, no. 2, 2002.

[7] O. Birgul, B. M. Eyuboglu, and Y. Z. Ider, "Current constrained voltage scaled reconstruction (CCVSR) algorithm for MR-EIT and its performance with different probing current patterns," *Phys. Med. Biol.*, vol. 48, pp. 653-671, 2003.

[8] O. Kwon, J. Y. Lee, and J. R. Yoon, "Equipotential line method for magnetic resonance electrical impedance tomography," *Inverse Problems*, vol. 18, pp. 1089-1100, 2002.

[9] Y. Z. Ider and O. Birgul, "Use of the magnetic field generated by the internal distribution of injected currents for electrical impedance tomography

(MR-EIT)," *Elektrik*, vol. 6, pp. 215-225, 1998.

[10] O. Birgul, B. M. Eyuboglu, and Y. Z. Ider, "Experimental results for 2D magnetic resonance electrical impedance tomography (MR-EIT) using magnetic flux density in one direction," *Phys. Med. Biol.*, vol. 48, pp. 3485-3504, 2003.

[11] O. Birgul, M. Hamamura, L. Muftuler, and O. Nalcioglu, "Contrast and spatial resolution in MREIT using low amplitude current," *Phys. Med. Biol.*, vol. 51, pp. 5035-5049, 2006.

[12] Y. Z. Ider and S. Onart, "Algebraic reconstruction for 3D magnetic resonance-electrical impedance tomography (MREIT) using one component of magnetic flux density," *Physiol. Meas.*, vol. 25, pp. 281-294, 2004.

[13] S. H. Oh, B. I. Lee, E. J. Woo, S. Y. Lee, M. H. Cho, O. Kwon, and J. K. Seo, "Conductivity and current density image reconstruction using harmonic Bz algorithm in magnetic resonance electrical impedance tomography," *Phys. Med. Biol.*, vol. 48, pp. 3101-3116, 2003.

[14] H. J. Kim, Y. T. Kim, A. S. Minhas, W. C. Jeong, E. J. Woo, J. K. Seo, and O. J. Kwon, "In vivo high-resolution conductivity imaging of the human leg using MREIT: The first human experiment," *IEEE Trans. Med. Imaging.*, vol. 28, pp. 1681-1687, 2009.

[15] C. Park, O. Kwon, E. J. Woo, and J. K. Seo, "Electrical conductivity imaging using gradient Bz decomposition algorithm in magnetic resonance electrical impedance tomography (MREIT)," *IEEE Trans. Med. Imaging.*, vol. 23, pp. 388-394, 2004.

[16] N. Gao, S. A. Zhu, and B. He, "A new magnetic resonance electrical impedance tomography (MREIT) algorithm: the RSM-MREIT algorithm with applications to estimation of human head conductivity," *Phys. Med. Biol.*, vol. 51, pp. 3067-3083, 2006.

[17] B. M. Eyuboglu, V. E. Arpinar, and R. Boyacioglu, "Comparison of magnetic resonance electrical impedance tomography (MR-EIT) reconstruction algorithms," *7th IEEE International Symposium on Biomedical Imaging: From Nano to Macro*, Rotterdam, pp. 700-703, 2010.

[18] B. I. Lee, S. H. Oh, E. J. Woo, S. Y. Lee, M. H. Cho, O. Kwon, J. K. Seo, J. Y. Lee, and W. S. Baek, "Three-dimensional forward solver and its performance analysis for magnetic resonance electrical impedance tomography (MREIT) using recessed electrodes," *Phys. Med. Biol.*, vol. 48, pp. 1971-1986, 2003.

[19] G. Z. Xu, H. L. Wu, S. Yang, S. Liu, Y. Li, Q. X. Yang, W. L. Yan, and M. S. Wang, "3-D electrical impedance tomography forward problem with finite element method," *IEEE T. Magn.*, vol. 41, pp. 1832-1835, 2005.

[20] S. Gabriel, R. W. Lau, and C. Gabriel, "The dielectric properties of biological tissues: III. Parametric models for the dielectric spectrum of tissues," *Phys. Med. Biol.*, vol. 41, pp. 2271-2293, 1996.

[21] T. J. C. Faes, H. A. Meij, J. C. Munck, and R. M. Heethaar, "The electric resistivity of human tissues (100 Hz-10 MHz): A meta-analysis of review studies," *Physiol. Meas.*, vol. 20, no. 4, pp. R1-R10, Nov. 1999.

[22] R. Sadleir, S. Grant, S. U. Zhang, B. I. Lee, H. C. Pyo, S. H. Oh, C. Park, E. J. Woo, S. Y. Lee, O. Kwonand, and J. K. Seo, "Noise analysis in MREIT at 3 and 11 Tesla field strength," *Physiol. Meas.*, vol. 26, pp. 875-884, 2005.